Supporting Information

Theoretical Insights on the Possible Applications of Amidoxime-Based Adsorbents in Neptunium and Plutonium Separation

Yan-Mei Chen,[a] Cong-Zhi Wang,[b] Qun-Yan Wu,[b] Jian-Hui Lan,[b] Zhi-Fang Chai,[a,b] and Wei-Qun Shi*[b]*

[a]Engineering Laboratory of Advanced Energy Materials, Ningbo Institute of Industrial Technology, Chinese Academy of Sciences, Ningbo, Zhejiang, 315201, China

[b]Laboratory of Nuclear Energy Chemistry, Institute of High Energy Physics, Chinese Academy of Sciences, Beijing 100049, China

*Email: shiwq@ihep.ac.cn; wangcongzhi@ihep.ac.cn

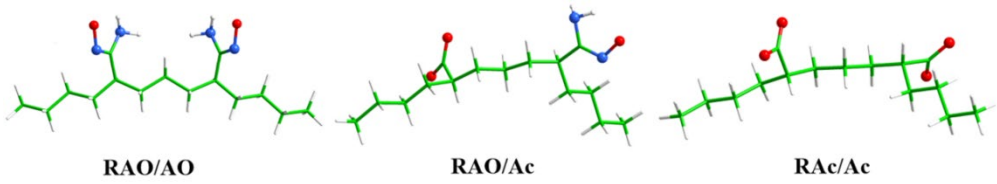

Figure S1. Optimized structures of the amidoxime/carboxyl-based adsorbents (R=$C_{13}H_{26}$). H, C, N, O atoms are represented by white, green, blue and red spheres, respectively. The subsequent figure adopt the same arrangement.

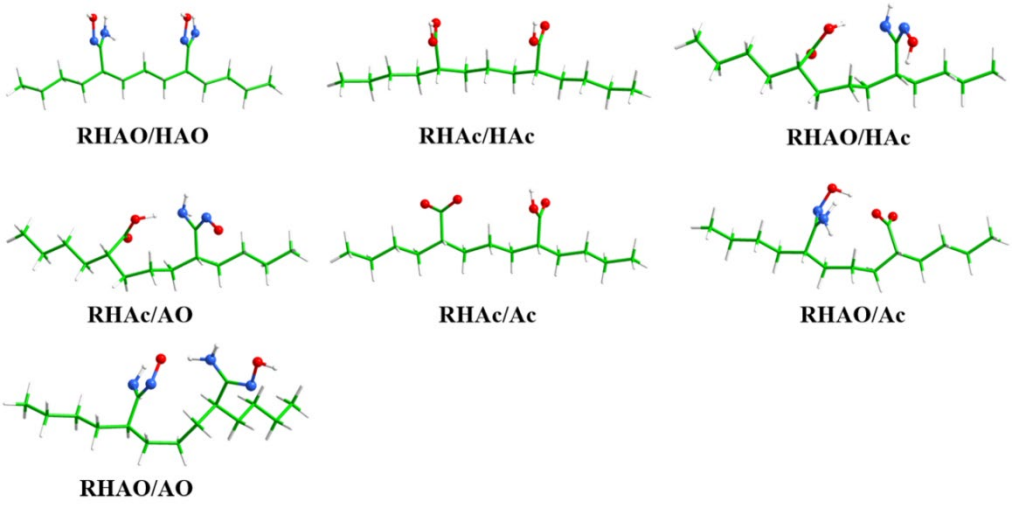

Figure S2. Optimized structures of the protonated amidoxime/carboxyl-based adsorbents.

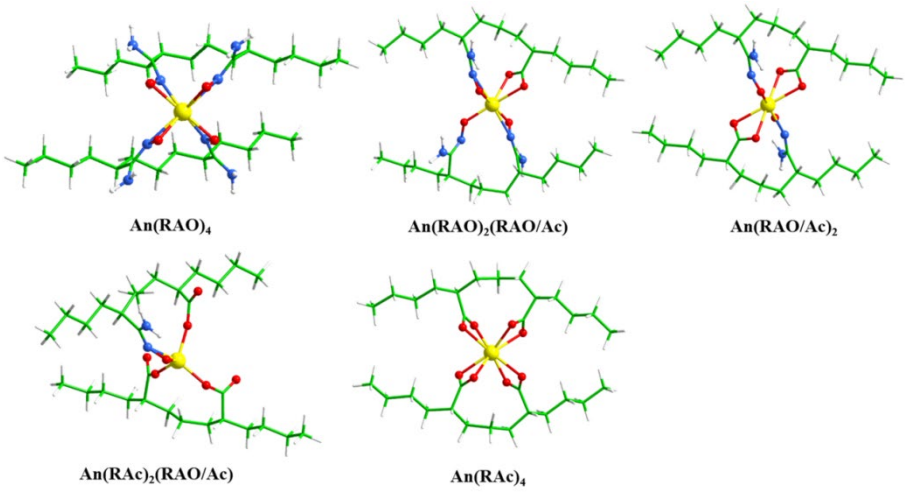

Figure S3. Optimized structures of the Np(IV) and Pu(IV) complexes with RAO^- and RAc^- by the B3LYP method. The H, C, N, O and actinide atoms are represented by white, green, blue, red and yellow spheres, respectively. The subsequent figures adopt the same arrangement.

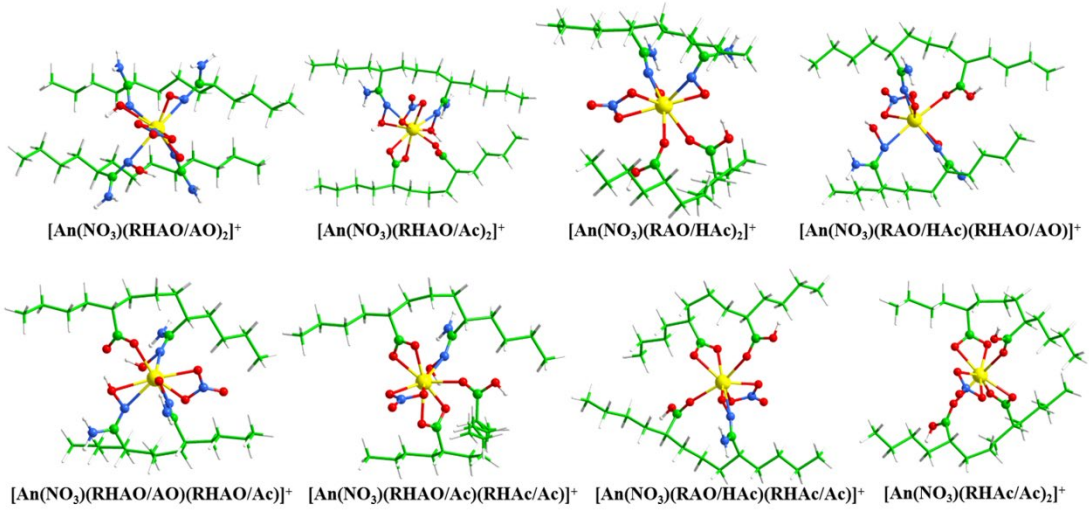

Figure S4. Optimized structures of the Np(IV) and Pu(IV) protonated complexes with RAO^-, RAc^-, and NO_3^- by the B3LYP method.

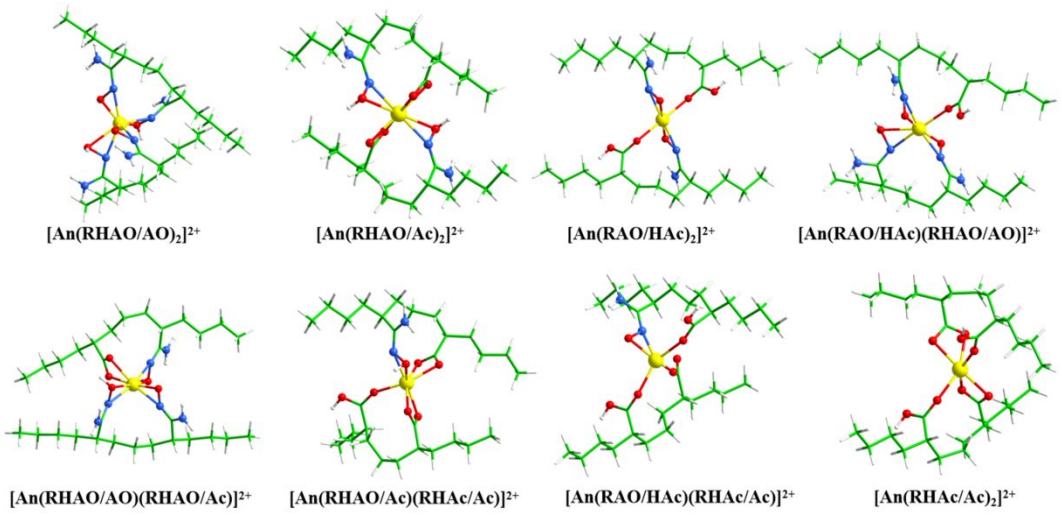

Figure S5. Optimized structures of the Np(IV) and Pu(IV) protonated complexes with RAO^- and RAc^- by the B3LYP method.

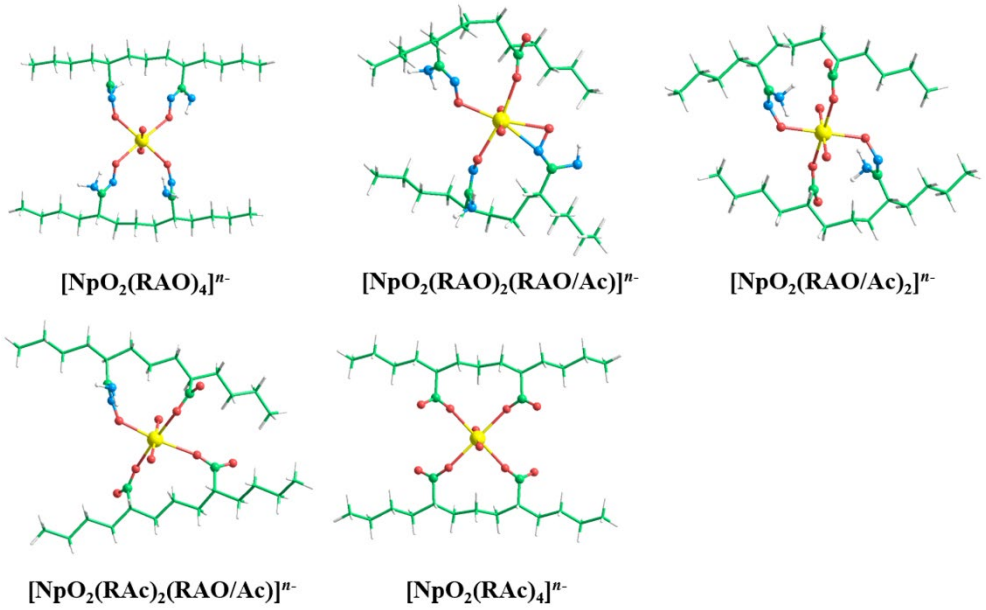

Figure S6. Optimized structures of Np(V, VI) complexes with RAO^- and RAc^- by the B3LYP method.

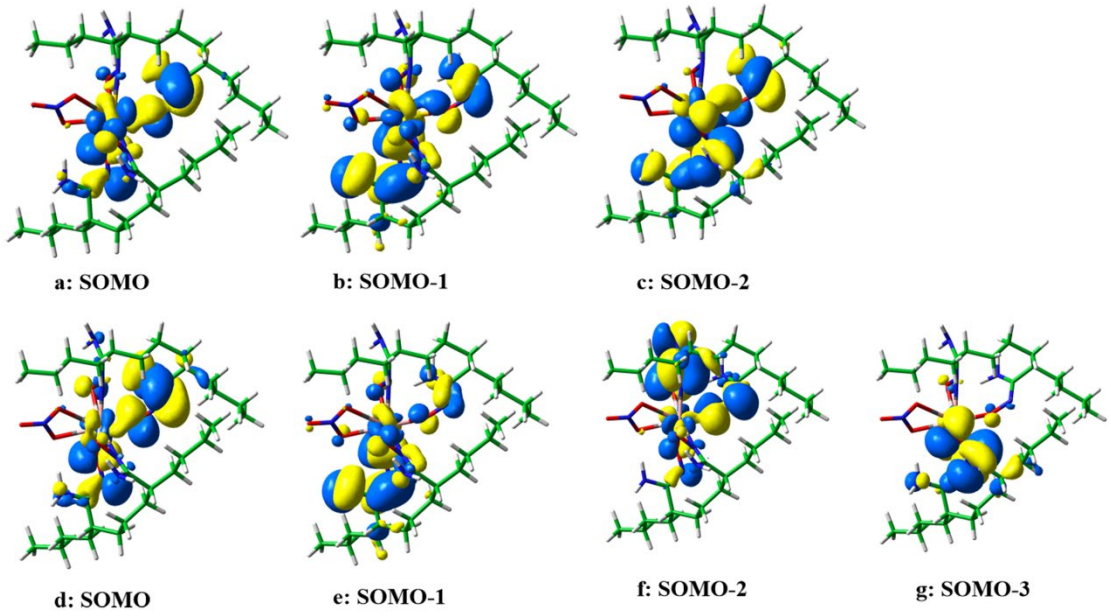

Figure S7. The α-spin valence MOs diagrams of the $[An(NO_3)(RAO)_4]^-$ complexes (a-c: Np; d-g: Pu) at the B3LYP/6-311G(d, p)/RECP level of theory (the isosurface value is set as 0.02 a.u.).

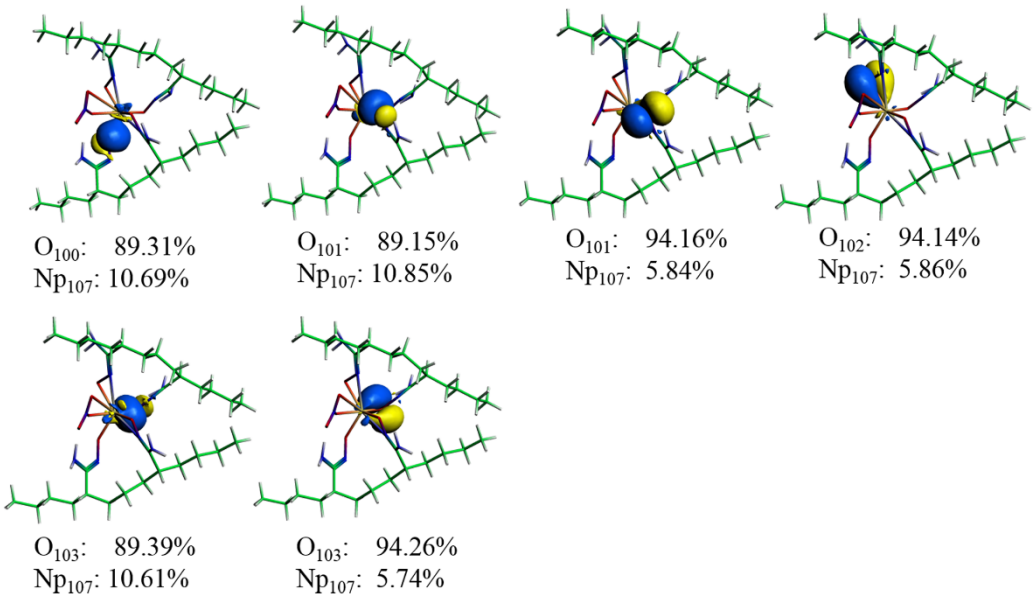

Figure S8. NBO σ and π orbitals of the Np-O bonds in $[Np(NO_3)(RAO)_4]^-$ calculated by the BP86 method.

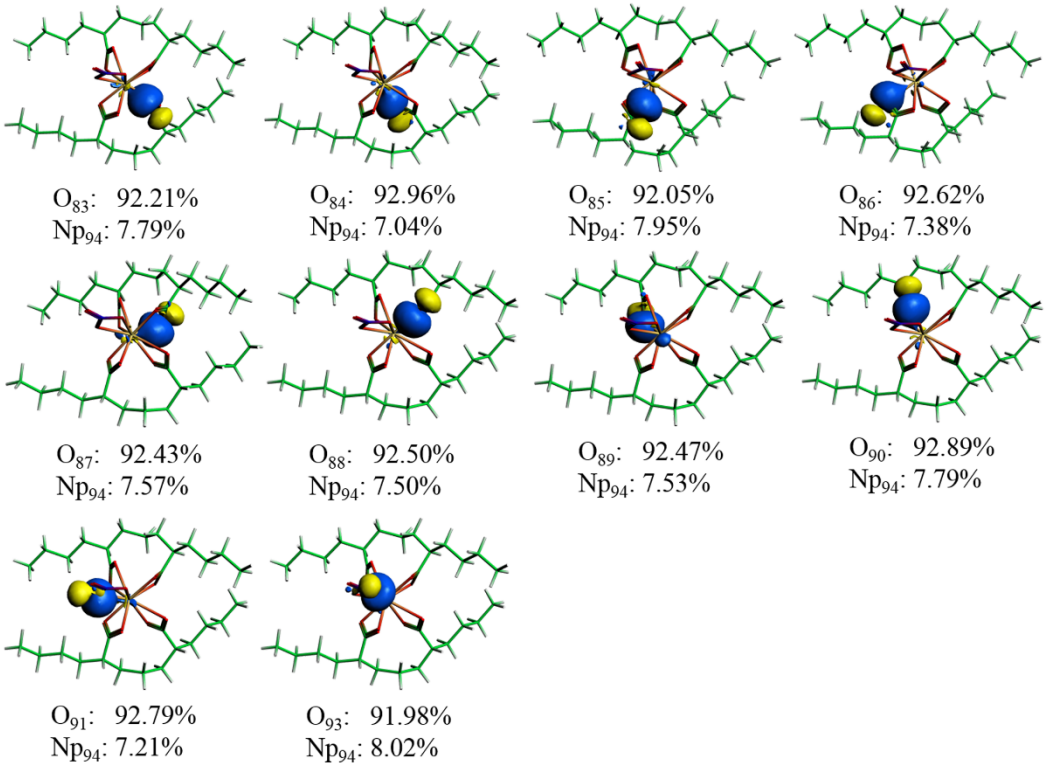

Figure S9. NBO σ orbitals of the Np-O bonds in $[Np(NO_3)(RAc)_4]^-$ calculated by the BP86 method.

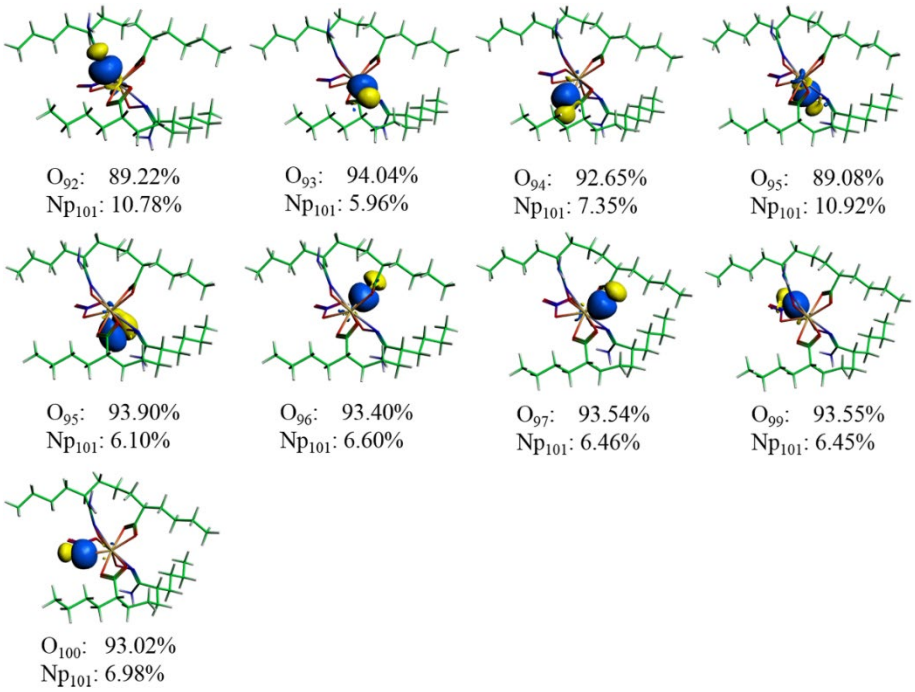

Figure S10. NBO σ and π orbitals of the Np-O bonds in $[Np(NO_3)(RAO/Ac)_2]^-$ calculated by the BP86 method.

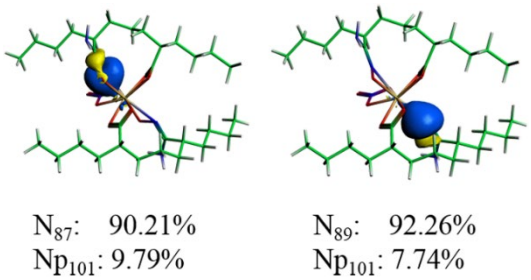

Figure S11. NBO σ orbitals of the Np-N bonds in $[Np(NO_3)(RAO/Ac)_2]^-$ calculated by the BP86 method.

Table S1. Bond Lengths (Å) for $[Pu^{IV}(HA)_3]^+$ Calculated by the B3LYP Method in Comparison with Experimental Data.

Species	Bond	Gas phase	Expt.
$[Pu^{IV}(HA)_3]^+$	Pu-O1	2.4074	2.3822(42)
	Pu-O2	2.3764	2.3727(44)
	Pu-O3	2.4089	2.4027(45)
	Pu-O4	2.3776	2.3765(48)
	Pu-O5	2.4132	2.3923(50)
	Pu-O6	2.3724	2.3593(57)
	Pu-N1	2.5199	2.4610(54)
	Pu-N2	2.5221	2.4741(58)
	Pu-N3	2.5193	2.4522(45)

Table S2. Np−N and Np−O Average Bond Lengths (Å) for the Np(V, VI) Complexes with RAO^-, RAc^- ($R=C_{13}H_{26}$) by the B3LYP Method. [a]

Species	Np-O(axial)	Np-O(RAc^-)	Np-O(RAO^-)	Np-N(RAO^-)
$[NpO_2(RAO)_4]^{n-}$	1.832/1.785	—	2.509/2.318	—
$[NpO_2(RAO)_2(RAO/Ac)]^{n-}$	1.835/1.785	2.572/2.442	2.547/2.378	2.630/2.561
$[NpO_2(RAO/Ac)_2]^{n-}$	1.840/1.780	2.544/2.391	2.421/2.294	—/2.849
$[NpO_2(RAc)_2(RAO/Ac)]^{n-}$	1.827/1.777	2.560/2.360	2.427/2.217	—
$[NpO_2(RAc)_4]^{n-}$	1.808/1.766	2.506/2.325	—	—

[a] ···/··· refers to the results for Np(V) and Np(VI) complexes, respectively.

Table S3. MBOs of Np-N and Np-O Bonds and Mulliken Charge Transfer (ΔQ_{Np}, *e*) from Ligands to Actinide Ions for the Np(V) and Np(VI) Complexes by the B3LYP Method. [a]

Species	Np-O (axial)	Np-O (RAc^-)	Np-O (RAO^-)	Np-N (RAO^-)	ΔQ_{Np}
$[NpO_2(RAO)_4]^{n-}$	2.087/2.109	—	0.338/0.525	—	3.907/4.648
$[NpO_2(RAO)_2(RAO/Ac)]^{n-}$	2.032/2.076	0.296/0.362	0.315/0.475	0.146/0.184	3.799/4.543
$[NpO_2(RAO/Ac)_2]^{n-}$	1.966/2.083	0.316/0.375	0.413/0.595	—/0.112	3.838/4.570
$[NpO_2(RAc)_2(RAO/Ac)]^{n-}$	2.014/2.093	0.297/0.401	0.434/0.726	—	3.793/4.552
$[NpO_2(RAc)_4]^{n-}$	2.110/2.137	0.262/0.426	—	—	3.806/4.518

[a] ···/··· refers to the results for Np(V) and Np(VI) complexes, respectively.

Table S4. Contribution (%) of Metal Atoms and the O/N of Amidoximate Group to the Delocalized Canonical MOs for Complexes $[An(NO_3)(RAO)_4]^-$ at the B3LYP/6-311G(d, p)/RECP Level of Theory.

Atoms	MO-192a	MO-193a	MO-194a	MO-198a
Np	5f:69.25	5f:43.66	5f:42.33	5f:35.24
	6d:1.30	6d:0.71	6d:1.43	—
$O(AO^-)$	2p:14.80	2p:23.53	2p:26.94	2p:29.95
$N(AO^-)$	2p:0.95	2p:8.82	—	—
$O(NO_3^-)$	—	—	—	—
Atoms	MO-193a	MO-194a	MO-195a	MO-199a
Pu	5f:31.31	5f:9.52	5f:11.62	5f:8.61
	6d:3.04	6d:2.62	6d:3.75	—
$O(AO^-)$	2p:39.10	2p:32.85	2p:28.74	2p:39.31
$N(AO^-)$	2p:8.64	2p:9.19	2p:1.52	—
$O(NO_3^-)$	—	—	—	—

Table S5. The Composition and Contribution of An and O Atomic Orbitals to Metal-Ligand Bonds for the $[Np(NO_3)(RAO)_4]^-$ calculated by the BP86 method.

Bonds	Bond Type	Np%	O%	Contribution of Np(%)	Contribution of O(%)
$Np_{107}–O_{100}$	π	10.69	89.31	7s(2.45)7p(0.13)6d(47.70)5f(49.72)	2s(21.92)2p(78.06)
$Np_{107}–O_{101}$	σ	10.85	89.15	7s(3.93)7p(0.21)6d(61.49)5f(34.38)	2s(29.21)2p(70.68)
$Np_{107}–O_{101}$	π	5.84	94.16	7s(0.09)7p(0.31)6d(27.22)5f(72.38)	2s(0.04)2p(99.82)
$Np_{107}–O_{102}$	π	5.86	94.14	7s(0.01)7p(0.35)6d(29.38)5f(70.25)	2s(0.14)2p(99.86)
$Np_{107}–O_{103}$	σ	10.61	89.39	7s(4.36)7p(0.30)6d(49.34)5f(46.00)	2s(30.16)2p(69.74)
$Np_{107}–O_{103}$	π	5.74	94.26	7s(1.94)7p(0.38)6d(37.76)5f(59.92)	2s(0.27)2p(99.61)

Table S6. The Composition and Contribution of An and O Atomic Orbitals to Metal-Ligand Bonds for the $[Np(NO_3)(RAc)_4]^-$ calculated by the BP86 method.

Bonds	Bond Type	Np%	O%	Contribution of Np(%)	Contribution of O(%)
$Np_{94}–O_{83}$	σ	7.79	92.21	7s(6.38)7p(1.68)6d(47.37)5f(44.58)	2s(21.91)2p(77.93)
$Np_{94}–O_{84}$	σ	7.04	92.96	7s(9.36)7p(1.84)6d(24.88)5f(63.91)	2s(19.57)2p(80.25)
$Np_{94}–O_{85}$	σ	7.95	92.05	7s(9.30)7p(0.55)6d(46.20)5f(43.95)	2s(23.06)2p(76.78)
$Np_{94}–O_{86}$	σ	7.38	92.62	7s(11.11)7p(1.41)6d(38.08)5f(49.40)	2s(18.96)2p(80.87)
$Np_{94}–O_{87}$	σ	7.57	92.43	7s(8.18)7p(1.16)6d(29.95)5f(60.71)	2s(21.50)2p(78.33)
$Np_{94}–O_{88}$	σ	7.50	92.50	7s(7.50)7p(1.56)6d(53.42)5f(37.52)	2s(20.60)2p(79.23)
$Np_{94}–O_{89}$	σ	7.53	92.47	7s(12.23)7p(1.36)6d(73.58)5f(12.83)	2s(21.82)2p(78.01)
$Np_{94}–O_{90}$	σ	7.79	92.89	7s(11.04)7p(1.26)6d(40.64)5f(47.06)	2s(20.51)2p(79.32)
$Np_{94}–O_{91}$	σ	7.21	92.79	7s(11.50)7p(1.66)6d(26.29)5f(60.55)	2s(26.59)2p(73.28)
$Np_{94}–O_{93}$	σ	8.02	91.98	7s(9.97)7p(1.08)6d(49.40)5f(39.55)	2s(30.34)2p(69.54)

Table S7. The Composition and Contribution of An and O Atomic Orbitals to Metal-Ligand Bonds for the $[Np(NO_3)(RAO/Ac)_2]^-$ calculated by the BP86 method.

Bonds	Bond Type	Np%	O/N%	Contribution of Np(%)	Contribution of O/N(%)
$Np_{101}–O_{92}$	σ	10.78	89.22	7s(6.17)7p(1.17)6d(44.30)5f(48.36)	2s(29.43)2p(70.44)
$Np_{101}–O_{93}$	π	5.96	94.04	7s(8.10)7p(7.92)6d(42.28)5f(41.70)	2s(16.96)2p(82.87)
$Np_{101}–O_{94}$	π	7.35	92.65	7s(11.34)7p(6.02)6d(44.99)5f(37.65)	2s(22.26)2p(77.59)
$Np_{101}–O_{95}$	σ	10.92	89.08	7s(7.71)7p(0.46)6d(41.96)5f(49.87)	2s(30.84)2p(69.05)
$Np_{101}–O_{95}$	π	6.10	93.90	7s(0.23)7p(4.63)6d(42.55)5f(52.58)	2s(0.35)2p(99.50)
$Np_{101}–O_{96}$	σ	6.60	93.40	7s(11.83)7p(6.98)6d(36.30)5f(44.89)	2s(19.61)2p(80.23)
$Np_{101}–O_{97}$	σ	6.46	93.54	7s(9.03)7p(8.75)6d(44.68)5f(37.54)	2s(18.89)2p(80.94)
$Np_{101}–O_{99}$	π	6.45	93.55	7s(10.53)7p(5.83)6d(43.98)5f(39.67)	2s(23.43)2p(76.44)
$Np_{101}–O_{100}$	σ	6.98	93.02	7s(11.09)7p(9.31)6d(41.49)5f(38.11)	2s(28.33)2p(71.55)
$Np_{101}–N_{87}$	π	9.79	90.21	7s(10.99)7p(1.83)6d(44.83)5f(42.35)	2s(40.53)2p(59.43)
$Np_{101}–N_{89}$	σ	7.74	92.26	7s(11.31)7p(4.72)6d(37.52)5f(46.46)	2s(40.31)2p(59.64)

Table S8. The Averaged Values are Presented for the Np–N and Np–O Bond Critical Points (BCPs) of the Np(V) Complexes by the B3LYP Method.

Species	Bonds	ρ	$\nabla^2\rho$	H
$[NpO_2(RAc)_4]^{3-}$	Np-O (axial)	0.135	0.321	-0.2092005
	Np-O (RAc^-)	0.022	0.195	0.0016439
$[NpO_2(RAO)_4]^{3-}$	Np-O (axial)	0.127	0.337	-0.1851091
	Np-O (RAO^-)	0.024	0.189	-0.0005280
	Np-N (RAO^-)	—	—	—
$[NpO_2(RAO)_3(RAc)]^{3-}$	Np-O (axial)	0.126	0.322	-0.1814755
	Np-O (RAc^-)	0.019	0.160	0.0016236
	Np-O (RAO^-)	0.022	0.168	-0.0001953
	Np-N (RAO^-)	0.018	0.145	0.0004947
$[NpO_2(RAO/Ac)_2]^{3-}$	Np-O (axial)	0.125	0.342	-0.1778992
	Np-O (RAc^-)	0.021	0.175	0.0008711
	Np-O (RAO^-)	0.030	0.233	-0.0027594
	Np-N (RAO^-)	—	—	—
$[NpO_2(RAO)(RAc)_3]^{3-}$	Np-O (axial)	0.129	0.316	-0.1899827
	Np-O (RAc^-)	0.019	0.168	0.0017864
	Np-O (RAO^-)	0.028	0.226	-0.0019836
	Np-N (RAO^-)	—	—	—

Table S9. The Averaged Values are Presented for the Np–N and Np–O Bond Critical Points (BCPs) of the Np(VI) Complexes by the B3LYP Method.

Species	Bonds	ρ	$\nabla^2\rho$	H
$[NpO_2(RAc)_4]^{2-}$	Np-O (axial)	0.150	0.323	-0.2591710
	Np-O (RAc^-)	0.035	0.287	-0.0048011
$[NpO_2(RAO)_4]^{2-}$	Np-O (axial)	0.143	0.333	-0.2346091
	Np-O (RAO^-)	0.038	0.281	-0.0078476
	Np-N (RAO^-)	—	—	—
$[NpO_2(RAO)_3(RAc)]^{2-}$	Np-O (axial)	0.143	0.329	-0.2347635
	Np-O (RAc^-)	0.027	0.218	-0.0007618
	Np-O (RAO^-)	0.034	0.236	-0.0061599
	Np-N (RAO^-)	0.024	0.194	-0.0023187
$[NpO_2(RAO/Ac)_2]^{2-}$	Np-O (axial)	0.145	0.328	-0.2412785
	Np-O (RAc^-)	0.030	0.247	-0.0018854
	Np-O (RAO^-)	0.042	0.287	-0.0125506
	Np-N (RAO^-)	—	—	—
$[NpO_2(RAO)(RAc)_3]^{2-}$	Np-O (axial)	0.146	0.326	-0.2454565
	Np-O (RAc^-)	0.032	0.268	-0.0026094
	Np-O (RAO^-)	0.049	0.344	-0.0179370
	Np-N (RAO^-)	—	—	—

Table S10. The Gibbs free energy changes (ΔG, kcal/mol) and the differences in ΔG (denoted as ΔΔG, kcal/mol) for the Reactions of Np(IV) and Pu(IV) Complexes with RAO^-, RAc^- ($R=C_{13}H_{26}$) in the Octanol Solution. [a]

Reactions	ΔG	ΔΔG
$[An(H_2O)_9]^{4+} + 2[RAO]_2^{2-} \rightarrow An(RAO)_4 + 9H_2O$	-236.7/-243.4	-6.7
$[An(H_2O)_9]^{4+} + [RAO]_2^{2-} + [RAO/Ac]^{2-} \rightarrow An(RAO)_2(RAO/Ac) + 9H_2O$	-212.0/-221.7	-9.7
$[An(H_2O)_9]^{4+} + 2[RAO/Ac]^{2-} \rightarrow An(RAO/Ac)_2 + 9H_2O$	-193.9/-194.8	-0.9
$[An(H_2O)_9]^{4+} + [RAO/Ac]^{2-} + [RAc]_2^{2-} \rightarrow An(RAc)_2(RAO/Ac) + 9H_2O$	-152.5/-163.1	-8.8
$[An(H_2O)_9]^{4+} + 2[RAc]_2^{2-} \rightarrow An(RAc)_4 + 9H_2O$	-144.8/-150.6	-5.8

[a] …/… refers to the results for Np(IV) and Pu(IV) complexes, respectively.

Table S11. The Gibbs free energy changes (ΔG, kcal/mol) and the differences in ΔG (denoted as ΔΔG, kcal/mol) for the Reactions of Np(IV) and Pu(IV) Complexes with RAO^-, RAc^- ($R=C_{13}H_{26}$), and NO_3^- in the Octanol Solution. [a]

Reactions	ΔG	ΔΔG
$[An(H_2O)_9]^{4+} + 2[RAO]_2^{2-} + NO_3^- \rightarrow [An(NO_3)(RAO)_4]^- + 9H_2O$	-226.5/-231.5	-4.9
$[An(H_2O)_9]^{4+} + [RAO]_2^{2-} + [RAO/Ac]^{2-} + NO_3^- \rightarrow [An(NO_3)(RAO)_2(RAO/Ac)]^- + 9H_2O$	-217.8/-225.5	-7.7
$[An(H_2O)_9]^{4+} + 2[RAO/Ac]^{2-} + NO_3^- \rightarrow [An(NO_3)(RAO/Ac)_2]^- + 9H_2O$	-200.5/-207.1	-6.6
$[An(H_2O)_9]^{4+} + [RAO/Ac]^{2-} + [RAc]_2^{2-} + NO_3^- \rightarrow [An(NO_3)(RAc)_2(RAO/Ac)]^- + 9H_2O$	-163.1/-170.2	-7.1
$[An(H_2O)_9]^{4+} + 2[RAc]_2^{2-} + NO_3^- \rightarrow [An(NO_3)(RAc)_4]^- + 9H_2O$	-151.7/-156.3	-4.6

[a] …/… refers to the results for Np(IV) and Pu(IV) complexes, respectively.

Table S12. The Gibbs free energy changes (ΔG, kcal/mol) and the differences in ΔG (denoted as ΔΔG, kcal/mol) for the Reactions of Np (V, VI) Complexes with RAO^- and RAc^- in the Octanol Solution.

Reactions	ΔG	ΔΔG
$[NpO_2(H_2O)_5]^+ + 2[RAO]_2^{2-} \rightarrow [NpO_2(RAO)_4]^{3-} + 5H_2O$	-75.4	-83.6
$[NpO_2(H_2O)_5]^{2+} + 2[RAO]_2^{2-} \rightarrow [NpO_2(RAO)_4]^{2-} + 5H_2O$	-159.0	
$[NpO_2(H_2O)_5]^+ + [RAO]_2^{2-} + [RAO/Ac)]^{2-} \rightarrow [NpO_2(RAO)_2(RAO/Ac)]^{3-} + 5H_2O$	-57.6	-77.8
$[NpO_2(H_2O)_5]^{2+} + [RAO]_2^{2-} + [RAO/Ac)]^{2-} \rightarrow [NpO_2(RAO)_2(RAO/Ac)]^{2-} + 5H_2O$	-135.4	
$[NpO_2(H_2O)_5]^+ + 2[RAO/Ac]^{2-} \rightarrow [NpO_2(RAO/Ac)_2]^{3-} + 5H_2O$	-64.7	-55.2
$[NpO_2(H_2O)_5]^{2+} + 2[RAO/Ac]^{2-} \rightarrow [NpO_2(RAO/Ac)_2]^{2-} + 5H_2O$	-119.9	
$[NpO_2(H_2O)_5]^+ + [RAO/Ac]^{2-} + [RAc]_2^{2-} \rightarrow [NpO_2(RAc)_2(RAO/Ac)]^{3-} + 5H_2O$	-40.3	-67.5
$[NpO_2(H_2O)_5]^{2+} + [RAO/Ac]^{2-} + [RAc]_2^{2-} \rightarrow [NpO_2(RAc)_2(RAO/Ac)]^{2-} + 5H_2O$	-107.8	
$[NpO_2(H_2O)_5]^+ + 2[RAc]_2^{2-} \rightarrow [NpO_2(RAc)_4]^{3-} + 5H_2O$	-43.3	-49.9
$[NpO_2(H_2O)_5]^{2+} + 2[RAc]_2^{2-} \rightarrow [NpO_2(RAc)_4]^{2-} + 5H_2O$	-93.2	

Table S13. The Gibbs free energy changes (ΔG, kcal/mol) and the differences in ΔG (denoted as ΔΔG, kcal/mol) for the reactions of Np(IV) and Pu(IV) protonated complexes with RAO^{-}, RAc^{-} ($R=C_{13}H_{26}$) in the octanol solution.[a,b]

Reactions	ΔG	ΔΔG
$[An(H_2O)_9]^{4+} + 2[RHAO/HAO] \rightarrow [An(RHAO/AO)_2]^{2+} + 9H_2O + 2H^+$	-6.4/-8.9	-2.5
$[An(H_2O)_9]^{4+} + 2[RHAO/HAc] \rightarrow [An(RHAO/Ac)_2]^{2+} + 9H_2O + 2H^+$	5.0/2.7	-2.3
$[An(H_2O)_9]^{4+} + 2[RHAO/HAc] \rightarrow [An(RAO/HAc)_2]^{2+} + 9H_2O + 2H^+$	11.5/2.0	-9.5
$[An(H_2O)_9]^{4+} + [RHAO/HAc] + [RHAO/HAO] \rightarrow [An(RAO/HAc)(RHAO/AO)]^{2+} + 9H_2O + 2H^+$	5.9/-1.5	-7.4
$[An(H_2O)_9]^{4+} + [RHAO/HAO] + [RHAO/HAc] \rightarrow [An(RHAO/AO)(RHAO/Ac)]^{2+} + 9H_2O + 2H^+$	-2.1/-9.5	-7.4
$[An(H_2O)_9]^{4+} + [RHAO/HAc] + [RHAc/HAc] \rightarrow [An(RHAO/Ac)(RHAc/Ac)]^{2+} + 9H_2O + 2H^+$	15.3/8.1	-7.2
$[An(H_2O)_9]^{4+} + [RHAO/HAc] + [RHAc/HAc] \rightarrow [An(RAO/HAc)(RHAc/Ac)]^{2+} + 9H_2O + 2H^+$	27.6/16.7	-10.9
$[An(H_2O)_9]^{4+} + 2[RHAc/HAc] \rightarrow [An(RHAc/Ac)_2]^{2+} + 9H_2O + 2H^+$	28.8/25.4	-3.4

[a] …/… refers to the results for Np(IV) and Pu(IV) complexes, respectively.

[b] The experimental free energy of solvation (-263.982 kcal/mol) was adopted for H^+.